

Bond Character of Thiophene on Ge(100): Effects of Coverage and Temperature

Seok Min Jeon,[†] Soon Jung Jung,[†] Hyeong-Do Kim,[‡] Do Kyung Lim,[†] Hangil Lee,^{*,‡} and Sehun Kim^{*,†}

Department of Chemistry and School of Molecular Science (BK21), Korea Advanced Institute of Science and Technology, Daejeon 305-701, Republic of Korea, and Beamline Research Division, Pohang Accelerator Laboratory (PAL), POSTECH, Pohang, Kyongbuk 790-784, Republic of Korea

Received: July 6, 2006; In Final Form: August 21, 2006

We have studied the adsorption and decomposition of thiophene (C_4H_4S) on Ge(100) using scanning tunneling microscopy (STM), high-resolution core-level photoemission spectroscopy (HRPES), and density functional theory (DFT) calculation. Analysis of S $2p$ core-level spectra reveals three adsorption geometries, which we assign to a Ge–S dative bonding state, a $[4 + 2]$ cycloaddition bonding state, and a decomposed bonding state (desulfurization reaction product). Furthermore, we found that the number ratio of the three adsorption geometries depended on the molecular coverage and the annealing temperature. At low coverages, the kinetically favorable dative bonding state is initially formed at room temperature. As the molecular coverage increases, thermodynamically stable $[4 + 2]$ cycloaddition reaction products are additionally produced. In addition, we found that as the surface temperature increased, the $[4 + 2]$ cycloaddition reaction product either possibly desorbed as molecular thiophene or decomposed to form a metallocycle-like species ($C_4H_4Ge_2$) and a sulfide (Ge_2S). We systematically elucidate the changes in the bonding states of adsorbed thiophene on Ge(100) according to the thiophene coverage and annealing temperature.

I. Introduction

The adsorption of organic molecules on semiconductors such as Si, Ge, and C (diamond) has been a subject of great interest both from a fundamental science perspective and as a result of the potential industrial applications of such systems.^{1–3} In particular, the adsorption of unsaturated organic molecules has been intensively studied on account of the potential uses of organic–semiconductor hybrid structures in microelectronic technologies.⁴ Highly ordered organic molecular layers have been prepared on semiconductor surfaces, usually by a cycloaddition^{5–7} or Lewis acid–base reaction⁸ between the organic molecules and the reconstructed (100) surface dimers.⁹ However, because organic molecules can adsorb onto semiconductor (100) surfaces with various adsorption geometries, highly ordered molecular structures have been successfully prepared on semiconductor surfaces in only a few cases.^{5–9}

Because a thiophene molecule contains a sulfur atom and an aromatic ring, it can adsorb onto semiconductor (100) surfaces in a variety of ways. If the conjugated diene takes part in the reaction, thiophene can undergo a $[4 + 2]$ cycloaddition reaction similar to that observed for benzene adsorbed on a Ge(100) surface.⁶ On the other hand, a $[2 + 2]$ cycloaddition reaction may occur if only one of the double bonds participates in the reaction. Furthermore, if the lone-pair electron of the thiophene molecule is donated to the electron-deficient down-Ge atom, a Lewis acid–base reaction is predicted to occur, as observed for pyridine on Ge(100).⁸

The adsorbed state of thiophene on the Ge(100) surface was first investigated by Rousseau et al. using valence band

photoemission spectroscopy.¹⁰ On the basis of comparisons of valence band photoemission spectra between the gas-phase 2,5-dihydrothiophene molecule and the 2,5-dihydrothiophene-like adsorbate on a Ge(100) surface, the authors concluded that a thiophene molecule chemisorbs onto a Ge(100) surface dimer through the $[4 + 2]$ cycloaddition reaction. However, contrary to their results, we recently reported that, at low coverage and room temperature, thiophene has two distinctive adsorption structures: a dative bonding configuration and a $[4 + 2]$ cycloaddition reaction product.⁹ At low coverage, thiophene formed one-dimensional (1-D) molecular chain structures through Lewis acid–base reaction. Moreover, over 0.25 ML, thiophene was additionally adsorbed between the adjacent molecular chains through the $[4 + 2]$ cycloaddition reaction.

In the present work, we have systematically studied the adsorption and decomposition behavior of thiophene on Ge(100) as a function of the amount of adsorbed thiophene and annealing temperature, using high-resolution core-level photoemission spectroscopy (HRPES) and scanning tunneling microscopy (STM), as well as density functional theory (DFT) calculations.

II. Experimental and Computational Methods

A Ge(100) sample (p -type, $R = 0.10$ – 0.39Ω) was cleaved to a size of 2×10 mm and mounted between two tantalum foil clips for measurements. The Ge(100) surface was cleaned by several cycles of sputtering with 1-keV Ar^+ ions for 20 min at 700 K, followed by annealing at 900 K for 10 min. The cleanliness of the Ge(100)- 2×1 surface was checked using STM and low-energy electron diffraction (LEED). An infrared optical pyrometer was used to measure the temperature of the Ge(100) sample. Thiophene (C_4H_4S , 99% purity) was purchased from Aldrich, and it was further purified by several freeze–pump–thaw cycles to remove all dissolved gases prior to exposure to the Ge(100) surface. The thiophene was inserted

* Corresponding authors. E-mail: sehun-kim@kaist.ac.kr (Kim); easyscan@postech.ac.kr (Lee).

[†] Korea Advanced Institute of Science and Technology.

[‡] Pohang Accelerator Laboratory (PAL).

into the prep-chamber by a variable leak valve at room temperature. The purity of the thiophene was checked using mass spectrometry.

The STM work was performed in an ultrahigh vacuum (UHV) chamber at a base pressure below 2.0×10^{-10} Torr equipped with an OMICRON VT-STM instrument. All STM images were recorded at a sample voltage of $V_s = -2.0$ V with a tunneling current of $I_t = 0.1$ nA using electrochemically etched W-tips.

High-resolution core-level photoemission spectra were recorded using a soft X-ray beamline (3A1) at the Pohang Accelerator Laboratory. S 2*p* core-level spectra were obtained with a high-performance electron analyzer (SES-2002, Gamma Data, Sweden) using photon energies of 500 eV. The overall resolution was 0.25 eV for the S 2*p* spectra. The binding energies of the three core-level spectra were referenced to the clean Au 4*f* core-level spectrum with binding energy of 84.0 eV and its valence band (Fermi energy) for the same photon energy. The base pressure of the chamber was maintained at 7.0×10^{-11} Torr. All of the spectra were recorded in the normal emission mode. The photoemission spectra were carefully analyzed by a standard nonlinear least-squares fitting procedure using Voigt functions.¹¹ The Lorentzian width was 0.06 eV (S 2*p*).

All DFT calculations of adsorption energies and transition states were performed by employing the JAGUAR 4.2 software package using the hybrid density functional (DFT) method, including the Becke's 3-parameter nonlocal-exchange functional with the correlation functional of Lee–Yang–Parr (B3LYP).¹² In these calculations, we considered one-dimer (Ge_2H_{12}) and two-dimer ($\text{Ge}_{15}\text{H}_{16}$) cluster models. The geometries of important local minima on the potential energy surface were determined at the B3LYP/LACVP** level of theory. The LACVP** basis set is a mixed basis set that uses the LACVP basis set to describe the Ge atoms and the 6-31G basis set for the remaining atoms. Moreover, the LACVP basis set describes atoms beyond Ar in the periodic table using the Los Alamos effective core potentials developed by Hay and Wadt.¹³ All structures were fully optimized without geometrical constraints on the clusters. Their transition states were verified through frequency calculations of the optimized structure, and all reported energies were zero-point corrected.

III. Results

3.1. STM Study. Figure 1a–c shows filled-state STM images of Ge(100) surfaces exposed to 10–50 L of thiophene at room temperature. At 10 L exposure of thiophene (Figure 1a), the major adsorption feature is the dative bonding configuration (feature A) as we previously reported, and thiophene molecules that formed 1-D molecular chains.⁹ Interestingly, these chains do not form on adjacent Ge dimer rows, indicating that steric hindrance between chains prevents growth of molecular chains on neighboring rows. When the amount of thiophene was further increased up to 30 L (Figure 1b) and 50 L (Figure 1c), the resulting surfaces show not only the molecular chain structures on every second dimer row, but also additional bright and round-shaped structures (feature B) between the chains. Finally, we examine the effects of annealing temperature on the two structures. Figure 1d shows an STM image of the Ge(100) surface that was first exposed to 50 L of thiophene at room temperature and then annealed at 400 K for 5 min. In the STM image, after annealing at 400 K the molecular chain structures have fully been desorbed and the bright-dot protrusions remain. We therefore conclude that feature B is thermodynamically more stable than feature A. This annealing experiment result is very

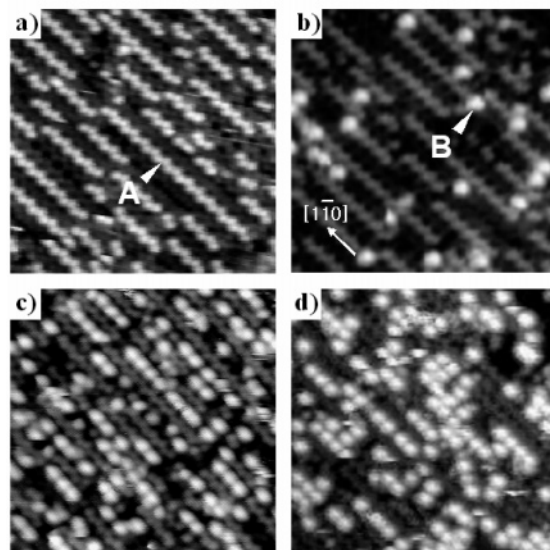


Figure 1. Filled-state STM images ($15 \times 15 \text{ nm}^2$, $V_s = -2.0$ V, $I_t = 0.1$ nA) of clean Ge(100) surfaces that have been exposed to (a) 10 L (0.21 ML), (b) 30 L (0.22 ML), and (c) 50 L (0.26 ML) of thiophene at room temperature. (d) Image taken after annealing the surface (c) at 400 K for 5 min.

consistent with the result in our earlier report⁹ where we assigned feature B to the $[4 + 2]$ cycloaddition reaction product which had stronger chemical bonding with a Ge(100) dimer than the dative bonding product (feature A).

To precisely determine the positions of each bright protrusion of feature A and feature B in the STM images, we examined line profiles of the STM images at two distinct coverages, 0.1 and 50 L (Figure 2). In the profile of the 0.1 L thiophene on the Ge(100) system (Figure 2a,b), the red curve indicates the cross section of the clean Ge(100) along the dimer row (aa'), and the vertical lines drawn through the peaks and troughs of the red curve indicate the positions of the Ge dimers. By superimposing the curve taken along the bare Ge substrate (aa') and the curves taken along a line containing adsorbed thiophene (bb'), we can compare the relative positions of feature A and the Ge dimers. As shown in Figure 2a,b, the bright protrusions of feature A are positioned above the locations in the middle of adjacent Ge atoms along the dimer row direction. Because there are no surface Ge atoms at the positions at which the protrusions of feature A are observed, we can clearly attribute the bright protrusions to thiophene molecules. This assignment is reasonable, given that other aromatic molecules such as styrene⁷ and pyridine⁸ appear as bright protrusions when adsorbed on Ge(100) surfaces. To check the position of feature B, we also examined line profiles for this feature, as shown in Figure 2c,d. In this case, different from the lines in Figure 2b, vertical lines through the peaks and troughs of the red curve (dd') indicate the positions of the protrusions of feature A, which are positioned above the locations in the middle of adjacent Ge atoms along the dimer row direction. Superposition of curves cc' and dd' reveals that the locations of feature B protrusions coincide with the midpoint of adjacent protrusions of feature A along the dimer row direction, indicating that the feature B protrusions are located on top of every second Ge dimer.

3.2. HRPES Study. To understand the coverage- and temperature-dependent nature of bond character of adsorbed thiophene on Ge(100), we investigated the S 2*p* core-level spectra of the adsorbed thiophene on a Ge(100) surface using synchrotron radiation as a function of thiophene exposure and surface temperature. Figure 3a shows the S 2*p* core-level

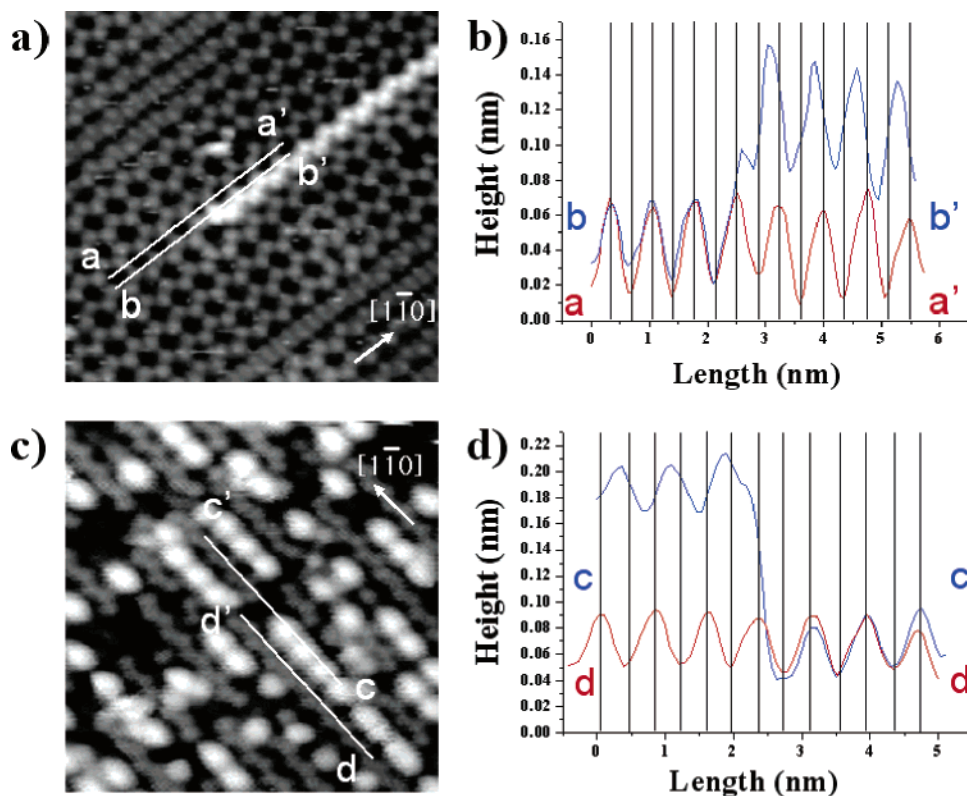


Figure 2. Filled-state STM images ($10 \times 10 \text{ nm}^2$, $V_s = -2.0 \text{ V}$, $I_t = 0.1 \text{ nA}$) of thiophene adsorbed on Ge(100) after exposure to (a) 0.1 L (0.02 ML) or (c) 50 L (0.26 ML) of thiophene. (b) and (d) show cross-section line profiles along $[1\bar{1}0]$ in (a) and (c), respectively.

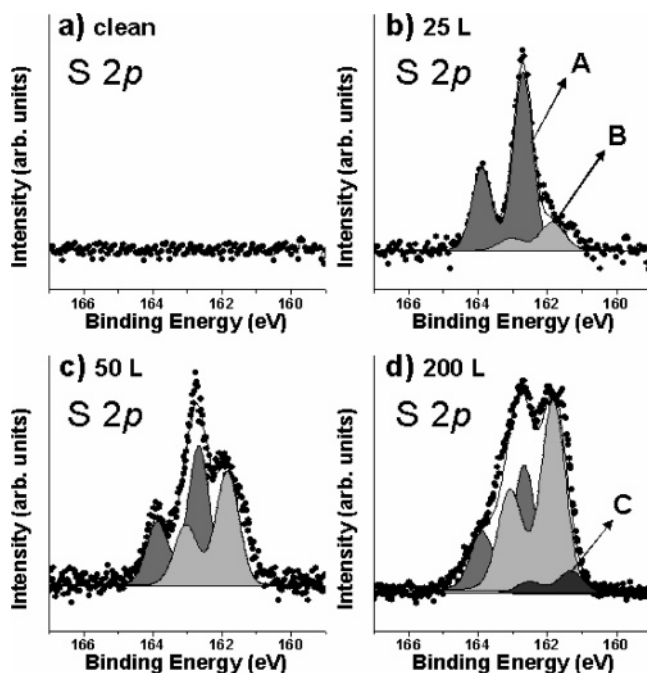


Figure 3. $S\ 2p$ core-level spectra of (a) a clean Ge(100) surface; and thiophene on Ge(100) systems in which the Ge(100) surfaces were exposed to (b) 25 L (84:16:0), (c) 50 L (52:48:0), and (d) 200 L (35:58:7) of thiophene, respectively (values in parentheses correspond to area ratios). The dots are experimental values, and the solid lines represent the results of peak fitting.

spectrum obtained for a clean Ge(100) surface whose spectrum does not show any spectral features indicating that no impurities or residual gases were present. After confirming the cleanness of the Ge(100) surface, we exposed the surface to various amounts of thiophene at room temperature. Figure 3b–d shows the $S\ 2p$ core-level spectra taken after exposing a clean Ge(100)

surface to 25, 50, and 200 L of thiophene at room temperature. In the $S\ 2p$ core-level spectrum (Figure 3b), we could resolve two bonding features, one located at 162.7 eV (marked as A) and the other at 161.8 eV (marked as B).

Because of the lack of preceding studies about the binding energy of $S\ 2p$ when an S atom is bound to Ge atoms through either a Ge–S direct bonding or a Ge–C–S bonding, the assignment of $S\ 2p$ binding energy of our system was not so straightforward. However, since the binding energy for physisorbed thiophene on a metal surface at low temperature is usually around 164 eV,^{14–16} we can exclude the existence of the physisorbed thiophene. When the thiophene molecule is bound to the Ge atom via the stronger chemical bonding, the S atom withdraws electrons from the less electronegative Ge atom more strongly than the case for the weak electrostatic interaction in the Ge–S dative bond. This concept may not be easily accepted because the dative bonding configuration has a firsthand Ge–S bonding. However, as we elucidated through showing the optimized geometry and the adsorption energy using DFT calculations in our previous study,⁹ the bonding between Ge and S in this adsorption configuration is as weak as physisorption. The detailed instruction about structure and energy will be treated in the following DFT calculation section. Therefore, we assign these two peaks to the dative bonding state (A) and the $[4 + 2]$ cycloaddition bonding state (B), respectively. Moreover, the peak corresponding to the dative bonding state is more intense than that corresponding to the $[4 + 2]$ cycloaddition bonding state, indicating that the former state dominates at this coverage. Consistently, the STM image showed that a majority of thiophene molecules reacted with Ge(100) through the dative bonding when we exposed the surface to 30 L of thiophene (Figure 1b). To more precisely examine the changes in intensity among the bonding features as a function of thiophene coverage, we examined spectra

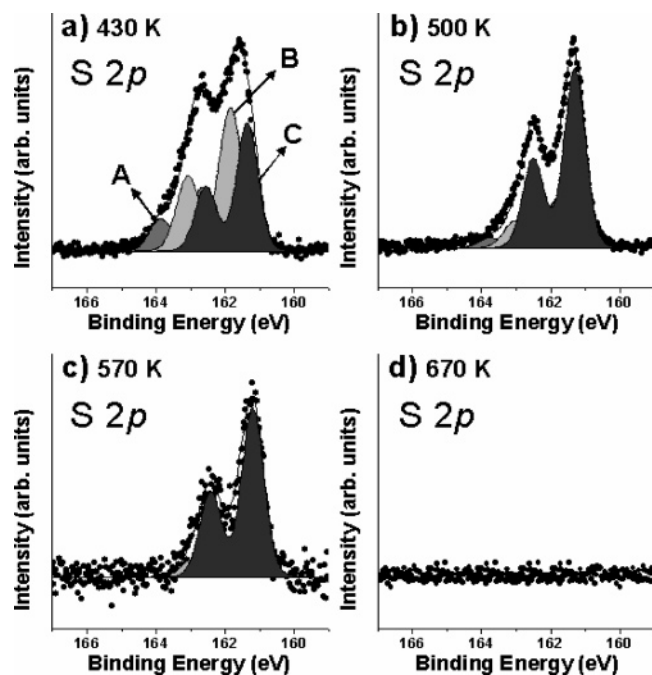


Figure 4. S 2*p* core-level spectra for thiophene on Ge(100) systems that were exposed a clean Ge(100) surface to 200 L of thiophene at room temperature, and followed by annealing for 5 min at (a) 430 K (19:44:37), (b) 500 K (8:21:70), (c) 570 K (0:18:82), and (d) 670 K, respectively (values in parentheses correspond to area ratios). The dots are experimental values, and the solid lines represent the results of peak fitting.

recorded at higher thiophene exposures. Figure 3c shows the S 2*p* core-level spectrum obtained after exposing a clean Ge(100) surface to 50 L of thiophene at room temperature. Comparison of these spectra with the spectra for 25 L exposure (Figure 3b) discloses that the intensity of the [4 + 2] cycloaddition bonding feature is largely enhanced, compared with the dative bonding feature, when the amount of thiophene is increased from 25 to 50 L, although the intensity of the dative bonding state is still larger at this coverage. Considering the variation of HRPES intensities of the two bonding states (Figure 3b,c) and the STM data at the thiophene exposure of 30 L (Figure 1b) and 50 L (Figure 1c), we confirm that the dative bonding state is dominant at this range of coverages. To clarify the variation of the two bonding states as a function of thiophene coverage and to confirm whether any other features emerge, we additionally conducted experiments in which a clean Ge(100) surface was exposed to 200 L of thiophene (Figure 3d). In this spectrum, despite the smallest intensity, we identified the appearance of a new bonding peak (marked as C) located at 161.2 eV (S 2*p*).

To monitor the change in the bonding features as a function of annealing temperature, we recorded a series of S 2*p* core-level spectra for Ge(100) surfaces that were first exposed to 200 L of thiophene at room temperature and then annealed for 5 min at 430 K (Figure 4a), 500 K (Figure 4b), 570 K (Figure 4c), or 670 K (Figure 4d). After annealing at 430 K (Figure 4a), the intensities of the [4 + 2] cycloaddition bonding state (B) and the bonding state C clearly increase, whereas the feature corresponding to the dative bonding state (A) decreases markedly compared to the spectra recorded prior to annealing. The changes among the bonding features observed in the core-level spectra thus indicate that the [4 + 2] cycloaddition bonding state and the bonding state C are thermodynamically favorable. Figure 4b shows the S 2*p* core-level spectra recorded after annealing the sample at 500 K for 5 min. In this spectrum, the bonding state C dominates, with the [4 + 2] cycloaddition

bonding state being remarkably decreased, and the feature associated with the dative bonding state (A) has almost disappeared. Thus, we can speculate that the [4 + 2] cycloaddition bonding feature will disappear if we increase the annealing temperature. After annealing the sample at 570 K for 5 min (Figure 4c), we found that the feature associated with the dative bonding state (A) had fully disappeared, the [4 + 2] cycloaddition bonding state (B) decreased slightly, and the bonding state C dominated. Finally, we examine the effect of annealing at 670 K for 5 min, which is known to be a germanium sulfide desorption temperature.^{16,17} Investigation of the S 2*p* core-level spectrum (Figure 4d) confirms that the bonding state C has fully disappeared. Therefore, because the bonding state C is the most thermodynamically stable, the S 2*p* binding energy is the lowest, and the desorption temperature is similar to a germanium sulfide desorption temperature, we suggest that the bonding state C is assigned to a germanium sulfide bonding state through a desulfurization reaction.

To elucidate the desulfurization mechanism from the [4 + 2] cycloaddition product to the germanium sulfide, we searched for the similar reaction on the Si(100) surface which has geometric and electronic structures similar to those of the Ge(100) surface. The decomposition mechanism of a [4 + 2] cycloaddition adduct to a Si₂S and a C₄H₄Si₂ at a thiophene on the Si(100) system has already been studied through experimental^{18–20} and theoretical²¹ methods. Among the studies performed to date, Lu et al.²¹ performed theoretical calculations on the thiophene on the Si(100) system using the hybrid density functional (B3LYP) method through a cluster model approach. They concluded that the [4 + 2] cycloaddition reaction was the most thermodynamically stable, and the [4 + 2] cycloaddition adduct could further undergo a desulfurization reaction by transferring a sulfur atom to a neighboring Si dimer.

3.3. DFT Calculation Study. On the basis of the earlier theoretical results for thiophene on Si(100),²¹ we suggest three possible adsorption structures for thiophene on Ge(100): a [2 + 2] cycloaddition adduct (Figure 5a), a [4 + 2] cycloaddition adduct (Figure 5b), and a Ge–S dative bonding adduct (Figure 5c). Of these three candidates, our DFT calculations showed that the [4 + 2] cycloaddition reaction product has the largest adsorption energy of −21.4 kcal/mol. In terms of the activation barriers, the [2 + 2] process has a transition state (Figure 5d) with a barrier height of 1.3 kcal/mol with respect to free thiophene and a Ge₉H₁₂ cluster, whereas a saddle point could not be identified for the [4 + 2] process, suggesting that this process may be concerted and barrierless. Therefore, we conclude that the [4 + 2] cycloaddition reaction is kinetically and thermodynamically favored over the [2 + 2] cycloaddition reaction, similar to the case of thiophene on Si(100). Among the three candidates, the Ge–S dative bonding adduct has the least stable adsorption geometry, with an adsorption energy of −6.2 kcal/mol and a Ge–S bond length of 2.697 Å predicted at the B3LYP/LACVP** level of theory (Figure 5c). However, we predict that from a kinetic standpoint, the Lewis acid–base reaction via Ge–S dative bonding may in fact be the most favorable reaction because it proceeds via an electrostatic attraction between an electron-deficient Ge dimer down-atom and nucleophilic lone-pair electrons of the sulfur atom without any significant activation energy such as bond breaking. The STM analysis presented above revealed that for thiophene coverages under 0.25 ML, a kinetically favorable molecular chain structure dominantly forms (Figure 1a,b). Moreover, we demonstrated that the protrusions comprising these chains were positioned above the locations in the middle of adjacent Ge

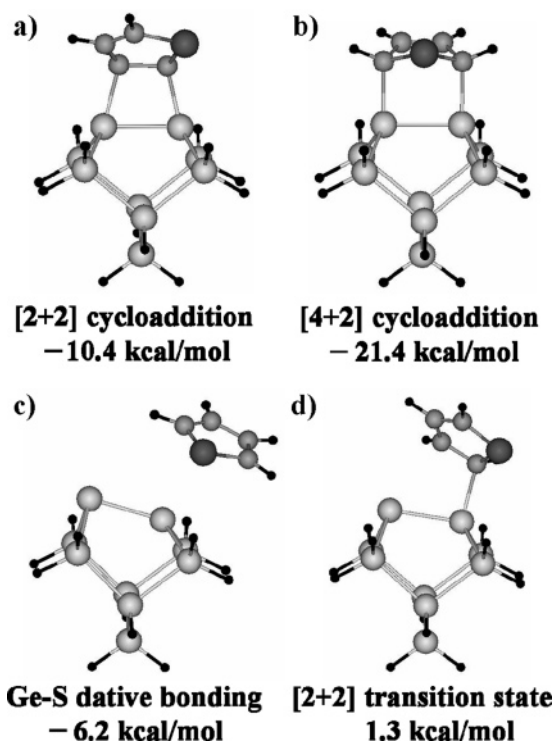


Figure 5. Local minima and a transition state for the thiophene on the Ge_9H_{12} system predicted at the B3LYP/LACVP** level of theory. Each value of (a), (b), and (c) is the adsorption energy (E_{ads}): $E_{\text{ads}} = E(\text{C}_4\text{H}_4\text{S on Ge}_9\text{H}_{12}) - E(\text{C}_4\text{H}_4\text{S}) - E(\text{Ge}_9\text{H}_{12})$ (in kcal/mol). The value of (d) is the activation energy of the [2 + 2] cycloaddition reaction with respect to a free thiophene and a Ge_9H_{12} cluster.

atoms along the dimer row direction (Figure 2a,b), in good agreement with the calculated geometry of the Ge–S dative bonding structure in Figure 5c. In the STM study, we also observed a second type of structure (feature B in Figure 1b) at higher thiophene coverages. This feature appeared on the STM image as round-shaped protrusions located on top of every second Ge dimer that were symmetric about the mirror plane containing the center of Ge dimer bonds (Figure 2c,d).

Moreover, further STM studies varying the surface temperature indicated that feature B was thermodynamically more stable than feature A. On the basis of these experimental results, we therefore assign feature B to the [4 + 2] cycloaddition adduct in Figure 5b.

When thiophene molecules adsorb onto a real Ge(100) surface via [4 + 2] cycloaddition, the thiophene molecules bind to every second dimer due to steric hindrance between the thiophene adsorbates. Therefore, further reactions with neighboring bare Ge dimers are possible. Figure 6 shows the potential energy surface for two reaction pathways of [4 + 2] cycloaddition adducts on $\text{Ge}_{15}\text{H}_{16}$ cluster models. In the desulfurization pathway, the sulfur atom of the [4 + 2] adduct migrates to the neighboring Ge dimer to form $\text{C}_4\text{H}_4\text{Ge}_2$ and Ge_2S . In the isomerization pathway, on the other hand, a [2 + 2] cycloaddition reaction occurs between the C=C bond of the [4 + 2] cycloaddition adduct and the neighboring Ge dimer.

In our calculations, when a thiophene molecule adsorbs onto a $\text{Ge}_{15}\text{H}_{16}$ cluster, two adsorption geometries can be considered (LM1 and LM2 in Figure 6). In the case of a real Ge(100) surface, however, the two adsorption models should be the same. Our calculations reveal that the adsorption energies for the two adsorption geometries are similar: -18.3 kcal/mol for LM1 and -18.5 kcal/mol for LM2. For the desulfurization process, the activation barrier is 20.5 kcal/mol with respect to the [4 + 2] cycloaddition adduct (LM1). The desulfurization product (LM3) lies at -42.3 kcal/mol with respect to the [4 + 2] cycloaddition adduct (LM1) and at -42.3 kcal/mol with respect to the entrance channel. For the isomerization process, on the other hand, the activation barrier is 22.0 kcal/mol with respect to the [4 + 2] adduct (LM2). The isomerization reaction product (LM4) has an adsorption energy of -0.9 kcal/mol with respect to the [4 + 2] cycloaddition adduct (LM2) and -19.4 kcal/mol with respect to the entrance channel. These data therefore indicate that the desulfurization process is thermodynamically and kinetically more favorable than the isomerization process. This theoretical observation is consistent with the HRPES results, which showed that the ratio of the decomposition bonding state (C) to the [4 + 2] cycloaddition bonding state (B) increased with increasing

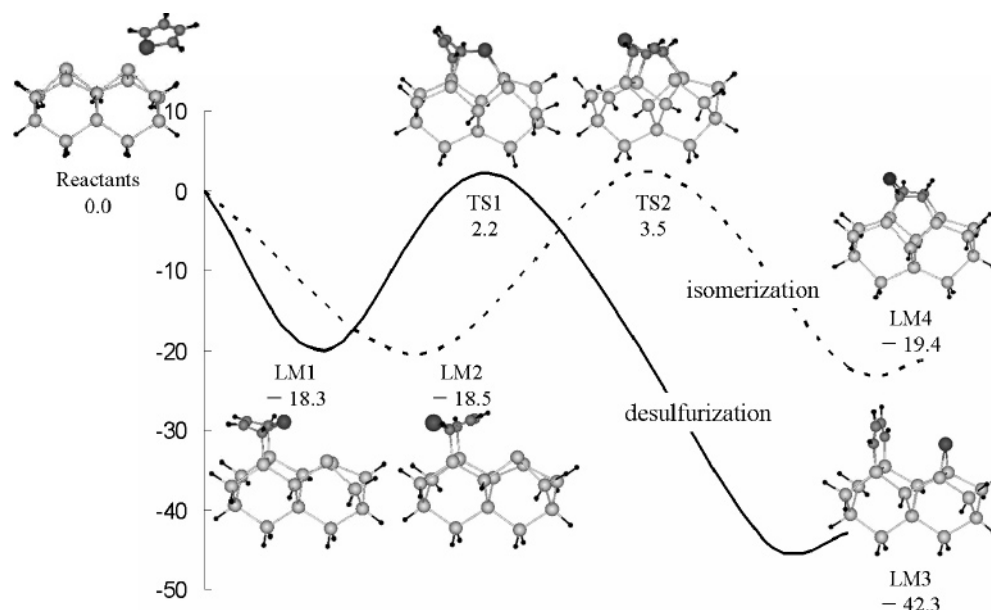


Figure 6. Calculated potential energy surface (PES) for the isomerization and desulfurization pathways of thiophene on $\text{Ge}_{15}\text{H}_{16}$ cluster models predicted at the B3LYP/LACVP** level of theory. The values cited are the adsorption energies with respect to the energies of free thiophene and the $\text{Ge}_{15}\text{H}_{16}$ cluster (in kcal/mol).

surface temperature. Therefore, we conclude that the desulfurization process takes place when the $[4 + 2]$ cycloaddition bonding state is thermally activated.

IV. Discussion

4.1. Difference between the Adsorption Structures of Thiophene on Si(100) and Those on Ge(100). The adsorption structures and thermal behavior of thiophene on Si(100) have been investigated by several groups. The data obtained in those studies indicate that, at room temperature, thiophene adsorbs onto the Si(100) surface through the $[4 + 2]$ cycloaddition reaction.^{10,19–21} Qiao et al. investigated the chemisorption and decomposition of thiophene on Si(100) using ultraviolet photoemission spectroscopy (UPS), X-ray photoelectron spectroscopy (XPS), and high-resolution electron energy loss spectroscopy (HREELS).¹⁹ They observed that thiophene was chemisorbed on Si(100) via the $[4 + 2]$ cycloaddition reaction at room temperature. Moreover, they concluded that above 400 K, the $[4 + 2]$ cycloaddition adduct desorbed or decomposed via two possible mechanisms: the formation of α -thiophenyl and Si–H, and the production of a metallocycle-like species and an atomic sulfur. On the basis of theoretical findings, Lu et al. suggested three possible adsorption structures: a $[2 + 2]$ cycloaddition reaction product, a $[4 + 2]$ cycloaddition reaction product, and a Ge–S dative bonding product.²¹ They concluded that the $[4 + 2]$ cycloaddition reaction was favored when thiophene adsorbed onto a Si(100) surface. Additionally, their calculations revealed that di- σ -bonded surface species formed by the $[4 + 2]$ process could undergo further $[2 + 2]$ cycloaddition with a neighboring Si dimer or desulfurization to form a metallocycle-like $C_4H_4Si_2$ species and a Si_2S .

Although the geometric and electronic structures of Si(100) and Ge(100) are similar, we observed that in addition to the bonding states observed for Si(100), there existed another bonding state for thiophene on Ge(100). This bonding state, which is observed at low thiophene coverage, is assigned to the Ge–S dative bonding state via the Lewis acid–base reaction. The observation of this additional bonding state, however, prompts the question of why the $[4 + 2]$ cycloaddition reaction is not facile at low coverages of thiophene on Ge(100), when the analogous reaction readily proceeds on Si(100).^{10,19–21} First, the $[4 + 2]$ cycloaddition reaction is kinetically much more unfavorable on Ge(100) than on Si(100). According to the symmetric reaction pathway, the $[4 + 2]$ cycloaddition reaction is allowed on a symmetric dimer with nearly zero activation energy. At room temperature, however, the most stable structure for Si(100) and Ge(100) is the buckled dimer conformation. On the basis of ab-initio calculations, the energy gap between the symmetric and buckled dimers is 3.228 kcal/mol for Si(100) and 6.918 kcal/mol for Ge(100).²² Thus, the overall activation energy that must be overcome for the $[4 + 2]$ reaction to proceed is equal to the energy difference between the buckled and symmetric dimers plus the activation energy for bond formation via the $[4 + 2]$ process. Konecny et al. employed a similar argument to explain the $[4 + 2]$ cycloaddition of 1,3-cyclohexadiene on Si(100); specifically, they insisted that the $[4 + 2]$ cycloaddition of 1,3-cyclohexadiene on Si(100) has an activation energy of less than 4 kcal/mol, which is the sum of the second-order saddle point energy for the $[4 + 2]$ process and the buckled-symmetric flipping energy of a Si(100) dimer.²³ Therefore, the reaction of thiophene with the Ge(100) surface via the $[4 + 2]$ process is kinetically very unfavorable compared to the Lewis acid–base reaction. Second, thiophene molecules gain extra stabilization energy when they align into molecular

chain structures on the Ge(100) surface rather than adsorb separately onto the surface via Ge–S dative bonding. This stabilization predominantly derives from the attractive π – π stacking interactions between stacked aromatic molecules in close proximity. For instance, in the case of two benzene molecules, the T-shaped structure and parallel-displaced structure are known to be the stable structures.^{24–26} Hunter et al. suggested that the stabilization enthalpy of a benzene dimer was in the range from -2.21 to -2.23 kcal/mol when two benzene molecules have “displaced-parallelled” configuration.²⁴ In the case of the thiophene adsorbate on Ge(100), our STM images showed the average distance between bright protrusions of dative bonding configurations (feature A) was around 0.41 nm (which was extremely close to intermolecular distances of similar π -stacked structures), 0.36–0.40 nm in the benzene dimer,²⁴ and 0.39–0.44 nm in the thiophene adsorbates on Au(111).¹⁵ We suppose that the Ge–S dative bonding is so weak that tilting of the Ge–S bond toward the center of the dimer row can occur to maximize the π – π stacking interaction. Consequently, considering reaction kinetics and additional stabilization energy, we conclude that Ge–S dative bonding configurations are favored at low coverages of thiophene on Ge(100).

4.2. Comparison between Bonding Configurations of Thiophene and Pyridine on Ge(100). A highly ordered organic molecular layer using pyridine molecules on Ge(100) was reported by Cho et al.⁸ They suggested that, under 0.25 ML, a highly ordered $c(4 \times 2)$ molecular layer was formed via Ge–N dative bonding between pyridine molecules and Ge(100) dimers. On the other hand, interestingly, under 0.25 ML, thiophene molecules create 1-D molecular chain structures on Ge(100), although they also utilize Ge–S dative bonding. The dissimilarity results from the different directions of lone-pair electrons on each heteroatom, nitrogen and sulfur. The sulfur atom in thiophene is sp^3 -hybridized, and therefore the lone-pair electrons are tilted away from the aromatic ring plane. As a consequence, when the thiophene molecule adsorbs onto a surface via the lone-pair electrons of the sulfur atom, the ring plane of the adsorbed thiophene is tilted with respect to the surface.^{27,28} In the case of a thiophene adsorbate on Ge(100), the adsorbed thiophene molecule is tilted with respect to the surface when it binds to the surface via Ge–S dative bonding. Moreover, the C_2 axis of the thiophene ring has a dihedral angle of 105.5° with respect to the Ge dimer bond (Figure 7a,b). Thus, we expect that thiophene molecules will adsorb onto the down-Ge atom with a “Gauche conformation”. This geometry is quite different from the conformation observed when a pyridine molecule, which has an sp^2 hybridized nitrogen atom with in-plane lone-pair electrons, adsorbs onto a Ge(100) surface (Figure 7c,d).⁸ Because the thiophene molecule has a “Gauche conformation” in the Ge–S dative bonding configuration, its ring would be expected to be positioned above the location in the middle of adjacent Ge atoms along the dimer row direction, which is in good agreement with the positions of the protrusions of feature A in the STM image (Figure 2a).

V. Conclusions

We have investigated the adsorption geometries and the coverage- and temperature-dependencies of the bonding states of thiophene adsorbed on a Ge(100) surface using HRPES and STM, and DFT calculations. We found that at room temperature, adsorption of thiophene at low coverages led to the formation of 1-D molecular chains of thiophene molecules on the Ge(100) surface via a kinetically favorable Lewis acid–base reaction. On increasing the coverage to over the theoretical saturation

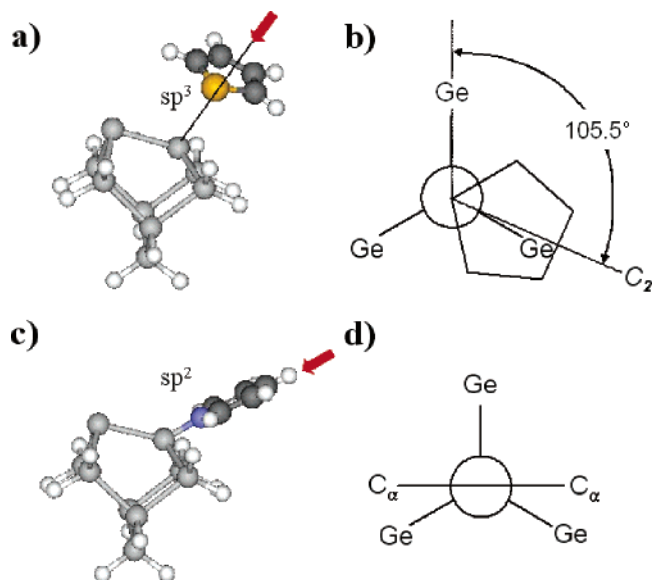


Figure 7. (a) Schematic models for dative bonding configurations of (a) thiophene and (c) pyridine on Ge(100). (b) and (d) are the Newman projections along the directions indicated by the red arrows in (a) and (c), respectively.

coverage of 0.25 ML, however, a thermodynamically stable $[4 + 2]$ cycloaddition adduct additionally appeared between adjacent molecular chains. Experiments examining the temperature dependence of the thiophene adsorption behavior on Ge(100) showed that as the temperature increased, the kinetically favorable Lewis acid–base reaction adducts first desorbed, followed by molecular desorption of the thermodynamically more stable $[4 + 2]$ cycloaddition reaction products or decomposition to form sulfur atoms and metallocycle-like species. Moreover, DFT calculations predicted that the $[4 + 2]$ cycloaddition reaction product is the thermodynamically most stable structure and that the $[4 + 2]$ cycloaddition adduct can further undergo desulfurization via sulfur atom migration to a neighboring Ge dimer.

Acknowledgment. This research was supported by the Brain Korea 21 project, the SRC programs (Center for Nanotubes and Nanostructured Composites and the Center for Strongly Correlated Material Research) of MOST/KOSEF, and the National

R & D Project for Nano Science and Technology. Additional support was provided by Grant No. KRF-2005-070-C00063 from the Korea Research Foundation, and Grant No. R01-2006-000-11247-0 from the the Basic Research Program of KOSEF (Dr. Lee).

References and Notes

- (1) Filler, M. A.; Bent, S. F. *Prog. Surf. Sci.* **2003**, 73, 1.
- (2) Yates, J. T. *Science* **1998**, 279, 335.
- (3) Amato, I. *Science* **1998**, 282, 402.
- (4) Wang, G. T.; Mui, C.; Musgrave, C. B.; Bent, S. F. *J. Am. Chem. Soc.* **2002**, 124, 8990.
- (5) Hamers, R. J.; Hovis, J. S.; Lee, S.; Liu, H.; Shan, J. *J. Phys. Chem. B* **1997**, 101, 1489.
- (6) Fink, A.; Menzel, D.; Widdra, W. *J. Phys. Chem. B* **2001**, 105, 3828.
- (7) Hwang, Y. J.; Kim, A.; Hwang, E. K.; Kim, S. *J. Am. Chem. Soc.* **2005**, 127, 5016.
- (8) Cho, Y. E.; Maeng, J. Y.; Hong, S.; Kim, S. *J. Am. Chem. Soc.* **2003**, 125, 7514.
- (9) Jeon, S. M.; Jung, S. J.; Lim, D. K.; Kim, H.-D.; Lee, H.; Kim, S. *J. Am. Chem. Soc.* **2006**, 128, 6296.
- (10) Rousseau, G. B. D.; Dhanak, V.; Kadodwala, M. *Surf. Sci.* **2001**, 494, 251.
- (11) Schreier, F. J. *Quant. Spectrosc. Radiat. Transfer* **1992**, 48, 743.
- (12) Lee, C.; Yang, W.; Parr, R. G. *Phys. Rev.* **1989**, B37, 785.
- (13) Hay, P. J.; Wadt, W. R. *J. Chem. Phys.* **1985**, 82, 299.
- (14) Göthelid, M.; Lelay, G.; Wigren, C.; Björkqvist, M.; Rad, M.; Darlsson, U. O. *Appl. Surf. Sci.* **1997**, 115, 87.
- (15) Noh, J.; Ito, E.; Nakajima, K.; Kim, J.; Lee, H.; Hara, M. *J. Phys. Chem. B* **2002**, 106, 7139.
- (16) Anderson, G. W.; Hanf, M. C.; Norton, P. R. *Appl. Phys. Lett.* **1995**, 66, 1123.
- (17) Nelen, L. M.; Fuller, K.; Greenlief, C. M. *Appl. Surf. Sci.* **1999**, 150, 65.
- (18) Jeong, H. D.; Lee, Y. S.; Kim, S. *J. Chem. Phys.* **1996**, 105, 5200.
- (19) Quao, M. H.; Cao, Y.; Tao, F.; Liu, Q.; Deng, J. F.; Xu, G. Q. *J. Phys. Chem. B* **2000**, 104, 11211.
- (20) Shimomura, M.; Ikejima, Y.; Yajima, K.; Yagi, T.; Goto, T.; Gunnella, R.; Abukawa, T.; Fukuda, Y.; Kono, S. *Appl. Surf. Sci.* **2004**, 237, 75.
- (21) Lu, X.; Xu, X.; Wang, N.; Zhang, Q.; Lin, M. C. *J. Phys. Chem. B* **2001**, 105, 10069.
- (22) Krüger, P.; Pollmann, J. *Phys. Rev. Lett.* **1995**, 74, 1155.
- (23) Konecny, R.; Doren, D. J. *J. Am. Chem. Soc.* **1997**, 119, 11098.
- (24) Hunter, C. A.; Singh, J.; Thornton, J. M. *J. Mol. Biol.* **1991**, 218, 837.
- (25) Hobza, P.; Selzle, H. L.; Schlag, E. W. *J. Am. Chem. Soc.* **1994**, 116, 3500.
- (26) Hobza, P.; Selzle, H. L.; Schlag, E. W. *J. Phys. Chem.* **1996**, 100, 18790.
- (27) Stöhr, J.; Gland, J. L.; Kollin, E. B.; Koestner, J.; Johnson, A. L.; Muetteries, E. L.; Sette, F. *Phys. Rev. Lett.* **1984**, 53, 2161.
- (28) Fulmer, J. P.; Zaera, F.; Tysoe, W. T. *J. Phys. Chem.* **1988**, 92, 4147.